TIME-DEPENDENT BEHAVIOR OF TRANSVERSE CRACKING IN CFRP CROSS-PLY LAMINATES

Keiji Ogi and Yoshihiro Takao

Research Institute for Applied Mechanics, Kyushu University
6-1, Kasuga-koen, Kasuga, Fukuoka 816-8580, Japan

SUMMARY: A model is developed to predict the transverse crack density and strain response in a cross-ply laminate under monotonic, bilinear and dead loading. First, the strain response of the cross-ply laminate with transverse cracking is presented based on the viscoelasticity theory and shear lag analysis. The transverse crack density is given as a function of both time and stress using a probabilistic failure concept. Secondly, monotonic tensile tests, bilinear tensile tests and dead load tests of cross-ply laminates are carried out to measure the strains and transverse crack density. Finally, the predicted strains and crack density are compared with the experimental ones to verify the validity of the present model. The present model provides good agreement with the experimental results.

KEYWORDS: transverse cracking, time-dependent, viscoelasticity, shear lag, probabilistic failure, creep

INTRODUCTION

Characterization of the long-term behavior of polymer composites is essential because of the time-dependent behavior of polymer matrix. In addition to the viscoelastic deformation, damages in composites are expected to increase with time under mechanical loading. Time-dependent behavior of deformation in composite materials has been studied mostly by means of a viscoelasticity theory[1-4] and viscoplasticity theory[5]. Development of transverse cracking in cross-ply laminates has been investigated by a shear lag analysis combined with statistical approaches[6-10].

On the other hand, time-dependent behavior of the transverse cracking has been investigated experimentally by Moore and Dillard[11] and Raghavan and Meshii[12]. Raghavan and Meshii[12] conducted constant strain rate and constant stress tests of AS4/3501-6 cross-ply laminates and have shown that matrix crack density and its rate of increase depend on strain rate and stress, respectively. However, any analytical model to predict the crack density with both time and stress has not been proposed.

In our previous paper[13], a creep model is developed for predicting the strain response of a cross-ply laminate where the transverse crack density increases with time under a constant stress. In the present paper, the model is modified and applied to the cases of both monotonic and bilinear loading. First, the strain response of a cross-ply laminate with transverse cracking is obtained using the viscoelasticity theory and shear lag analysis. The strain increments due to both viscoelastic deformation and transverse cracking are taken into

account in the model. The transverse crack density is given as a function of both time and stress using the time-dependent Weibull distribution function[14, 15]. Secondly, the monotonic tensile tests, bilinear tensile tests and dead load tests of $[0/90°_3]_S$ carbon/epoxy laminates are conducted to measure the strains and transverse crack density. A set of parameters for expressing the crack density is determined from the monotonic tensile tests at four different stress rates. Finally, the crack density and the strain response in both bilinear and dead load tests are predicted using the parameters and compared with the experimental ones to verify the present model.

MODELING

STRAIN RESPONSE

In order to obtain the strain and stress distributions in a cross-ply laminate with transverse cracking, a modified shear lag model[7, 9] is employed. It is assumed that first all the elastic moduli are functions of time while they are independent of the stress state, secondly the shear lag parameter α and residual thermal strains are independent of time, and thirdly no delamination occurs from a transverse crack tip. Fig. 1 shows a schematic drawing of crack spacing and strain as a function of time. When the strain vector at $t = t_k$ expressed by $\boldsymbol{\varepsilon}_k$ is given, the strain vector at $t = t_{k+1}$ is expressed as

$$\boldsymbol{\varepsilon}_{k+1} = \boldsymbol{\varepsilon}_k + \Delta\boldsymbol{\varepsilon}_k{}^C + \Delta\boldsymbol{\varepsilon}_{k+1}{}^D \tag{1}$$

where $\Delta\boldsymbol{\varepsilon}_k{}^C$ and $\Delta\boldsymbol{\varepsilon}_{k+1}{}^D$ are the strain increments due to applied load and transverse cracking, respectively, expressed as[13]

$$\Delta\boldsymbol{\varepsilon}_k{}^C = \boldsymbol{\varepsilon}^0(t_{k+1}) - \boldsymbol{\varepsilon}^0(t_k) + \{\boldsymbol{K}_1(t_{k+1}) - \boldsymbol{K}_1(t_k)\}\frac{\tanh(L_k\,\alpha)}{L_k\,\alpha} \tag{2}$$

$$\Delta\boldsymbol{\varepsilon}_{k+1}{}^D = \left\{\frac{\tanh(L_{k+1}\,\alpha)}{L_{k+1}\,\alpha} - \frac{\tanh(L_k\,\alpha)}{L_k\,\alpha}\right\}\boldsymbol{K}_2(t_{k+1}) \tag{3}$$

where $\boldsymbol{\varepsilon}^0(t)$ is the uniform mechanical strain, L_k is half length of crack spacing and $\boldsymbol{K}_1(t)$ and $\boldsymbol{K}_2(t)$ are functions of the relaxation moduli $Q_{ij}(t)$. Thus, the strain at an arbitrary time during $t_n \le t < t_{n+1}$ is obtained as

$$\boldsymbol{\varepsilon}(t) = \boldsymbol{\varepsilon}^0(t) + \boldsymbol{K}_1(t)\frac{\tanh(L_n\,\alpha)}{L_n\,\alpha} + \sum_{k=1}^{n}\left[\{\boldsymbol{K}_2(t_k) - \boldsymbol{K}_1(t_k)\}\left\{\frac{\tanh(L_k\,\alpha)}{L_k\,\alpha} - \frac{\tanh(L_{k-1}\,\alpha)}{L_{k-1}\,\alpha}\right\}\right] \tag{4}$$

The third term means the interference between viscoelastic deformation and progressive transverse cracking, which is negligible in the longitudinal direction by assuming the following equations[13]:

$$K_{1x}(t) = K_{2x}(t) = \frac{d}{b}\frac{\sigma_{x0}{}^{(2)}(t)}{Q_{11}{}^0} \equiv K_x(t)\,. \tag{5}$$

In addition, the continuous increase in the strain can be assumed if the crack density is given as a continuous function of time. Therefore, the longitudinal strain at an arbitrary time is derived from eqs. (4) and (5) as

$$\varepsilon_x(t,\sigma_x) = \varepsilon_x{}^0(t) + K_x(t)\frac{2\rho(t,\sigma_x)}{\alpha}\tanh\frac{\alpha}{2\rho(t,\sigma_x)} \tag{6}$$

where $\rho(t,\sigma_x)$ is the crack density which is the inverse of $2L(t,\sigma_x)$.

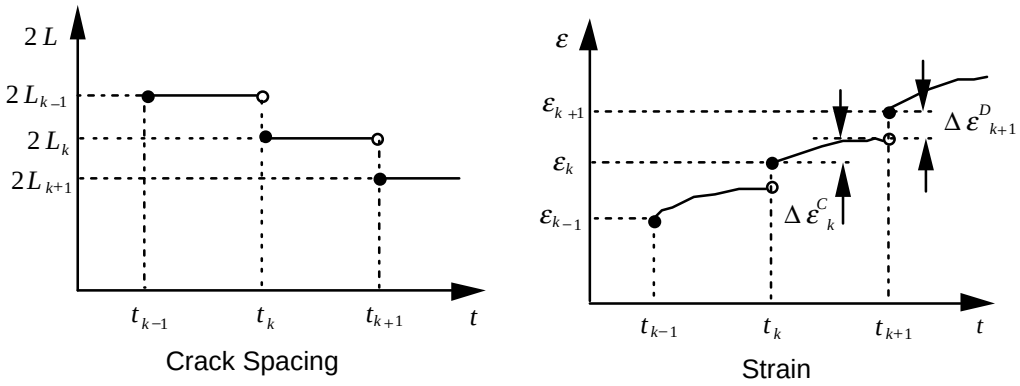

Fig. 1: Change in the crack spacing and strain with time in the present model.

TRANSVERSE CRACK DENSITY

Based on the probabilistic model associated with transverse cracking[6-8], it is assumed that a 90°-ply is divided into unit elements with a volume of V (length $2L$). Here we apply the time-dependent Weibull distribution[14, 15] to transverse cracking. The reliability probability function for transverse cracking is expressed as a function of time t and the 90°-ply stress $\sigma_x^{(2)}$ by

$$R(t,\sigma_x^{(2)}) = \exp\left\{-\int_V \Psi\left[\int_0^t \phi\left[\sigma_x^{(2)}\right]\, dt\right]\, dV\right\} \tag{7}$$

with

$$\Psi(\xi) = \alpha\,\xi^p\,, \quad \phi(\eta) = \beta\,\eta^q \tag{8}$$

where α, β, p and q are constants. $\sigma_x^{(2)}(x,t)$ is approximately expressed by

$$\sigma_x^{(2)}(x,t) = g(x)\,\sigma_x(t) \tag{9}$$

where $\sigma_x(t)$ is the laminate stress. Substituting eqs. (8) and (9) into eq. (7), we obtain

$$R(t,\sigma_x) = \exp\left\{-V_E\,\Psi\,\left[\int_0^t \phi\left[\sigma_x(t)\right]\, dt\right]\right\} \tag{10}$$

with

$$V_E = \frac{V}{L}\int_0^L \{g(x)\}^{pq}\, dx \tag{11}$$

where V_E is called as the effective volume. The transverse crack density is expressed as

$$\rho(t,\sigma_x) = \{1 - R(t,\sigma_x)\}\rho_s \tag{12}$$

where ρ_s is the saturation crack density.

First, the reliability probability function for monotonic loading is rewritten as

$$R_1(\sigma_x(t)) = \exp\left(-b\dot{\sigma}_x^{\,-n}\sigma_x(t)^{m+n}\right)$$

(13)

with

$$m = pq\,, \quad n = p\,, \quad b = \left(\frac{n}{m+n}\right)^n \alpha\,\beta^n\,V_E \tag{14}$$

where $\dot{\sigma}_x$ is a stress rate and b, m and n are empirically determined constants.

Next, for bilinear loading where the stress rate changes from $\dot{\sigma}_1$ to $\dot{\sigma}_2$ at a stress of σ^*, the reliability probability function is written as

$$R_2(\sigma_x(t)) = \begin{cases} \exp\left(-b\dot{\sigma}_1^{-n}\sigma_x(t)^{m+n}\right) & (0 < t < \sigma^*/\dot{\sigma}_1) \\ \exp\left[-b\left\{\sigma_x(t)^{\frac{m+n}{n}}/\dot{\sigma}_2 + \sigma^{*\frac{m+n}{n}}\left(1/\dot{\sigma}_1 - 1/\dot{\sigma}_2\right)\right\}^n\right] & (\sigma^*/\dot{\sigma}_1 \le t) \end{cases} \quad . \qquad (15)$$

Finally, the reliability probability function for dead loading is calculated as

$$R_3(t,\overline{\sigma}_x) = \lim_{\dot{\sigma}_2 \to 0} R_2(\sigma_x(t)) = \exp\left[-b\overline{\sigma}_x^{\,m}\left(\frac{m+n}{n}t - \frac{m\overline{\sigma}_x}{n\dot{\sigma}_x}\right)^n\right] \quad (\overline{\sigma}_x/\dot{\sigma}_x \le t) \qquad (16)$$

where $\dot{\sigma}_x$ and $\overline{\sigma}_x$ are an initial stress rate and a constant stress, respectively.

From eqs. (12) and (13), we obtain

$$Y = (m+n)X + \ln b \qquad (17)$$

with

$$X = \ln\sigma_x, Y = \ln\left\{\ln\left(\frac{\rho_S}{\rho_S - \rho}\right)\right\} + n\ln\dot{\sigma}_x \,. \qquad (18)$$

First, the values of Y are plotted against X for the monotonic tensile test at various stress rates. The value of n is determined so that the X-Y plots converges on one master line. Then, $m+n$ and $\ln b$ are obtained by least square fitting of the plots.

EXPERIMENTAL

Coupon specimens of $[0/90°_3]_S$ CF/Epoxy laminates (T800H/#3631, Toray) with the width of 8 mm were fabricated. The monotonic tensile, bilinear tensile and dead load tests were conducted at a temperature of 110°C to measure the strain and transverse crack density with time using an experimental setup shown in Fig. 2. Transverse cracking was monitored in-situ by a stereoscopic microscope and recorded by a VCR through a CCD camera. Transverse crack density was measured within the range of 60 mm length corresponding to the total gage length of the two strain gages. The time of transverse cracking was recognized with use of both the measured strain data and in-situ observation. The stress rates $\dot{\sigma}_x$, combinations of the stress rates $(\dot{\sigma}_1, \dot{\sigma}_2)$ and the stresses σ^* and $\overline{\sigma}_x$ are 0.8, 0.08, 0.008 and 0.0016 MPa/sec, (0.08, 0.0016) and (0.0016, 0.08) MPa/sec, σ^* = 480 and $\overline{\sigma}_x$ = 530 MPa, respectively. The parameters b, m and n were determined from the results of the monotonic tensile tests at four different stress rates using eq. (17). The shear lag parameter α was calculated from the strain increment due to transverse cracking during the creep tests, and the relaxation moduli $Q_{ij}(t)$ were determined from the creep test results of $[90°_8]$ specimens[13].

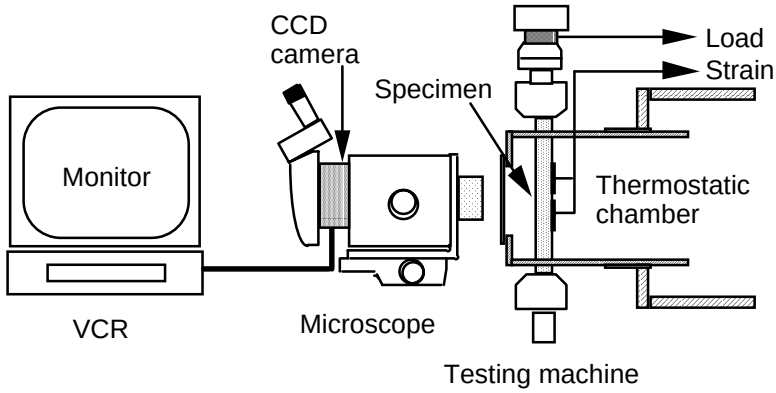

Fig.2: Experimental set-up for in-situ observation of transverse cracking during loading at a high temperature.

RESULTS AND DISCUSSION

Fig. 3 shows the effects of stress rates on the transverse crack density. The specimens for $\dot{\sigma}_x$ of 0.8, 0.08 and 0.008 MPa/sec were broken before the transverse crack density reached the saturation value (7 /cm). Remarkable rate-dependence is observed. In lower rates, first, the stress required for cracking decreases since the compliance of 90°-ply in the x direction increases, and secondly, delayed fracture occurs at a stress less than the quasi-static strength. From Figure 3, X and Y in eq. (18) are plotted in Fig. 4. The parameters obtained by these plots are presented in Table 1. The transverse crack densities represented using eq. (13) together with the above parameters are depicted as solid lines in Fig. 3.

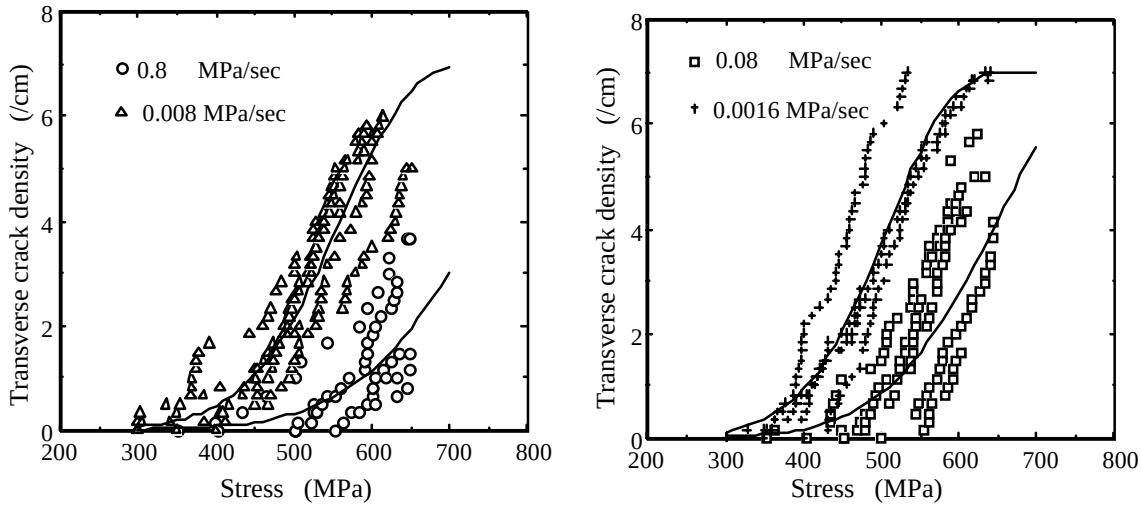

(a) (b)

Fig.3: Effects of stress rates on change in the transverse crack density in the monotonic tensile tests; (a) 0.8 and 0.008 MPa/sec and (b) 0.08 and 0.0016 MPa/sec.

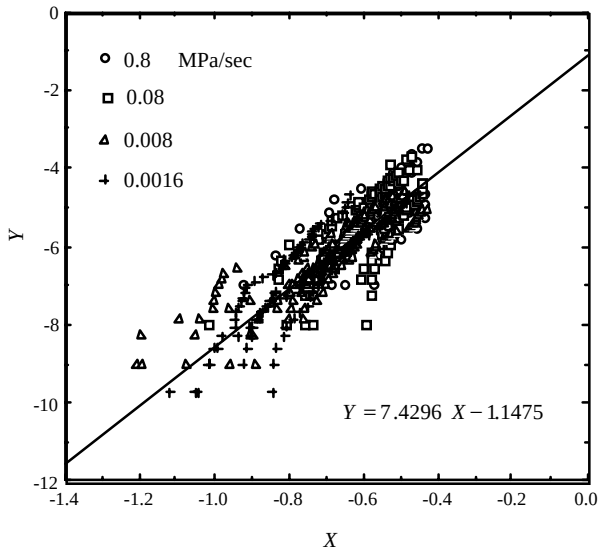

Fig. 4: The X-Y plots in eq. (17) for four different stress rates in the monotonic tensile tests. The solid line is obtained by least square fitting.

Table 1: The saturation crack density and parameters in eq. (14).

ρ_S (/cm)	7.0	m	6.98
b (GPa^{-m}sec^{-n})	0.317	n	0.450

Fig. 5 (a) shows the measured and predicted transverse crack density against stress in the bilinear tensile tests. The solid lines denote predictions for the bilinear tensile tests. A sudden increase in the crack density is observed when the stress rate changes from high to low ones, on the other hand, the crack density gradually approaches to the one of high rate when the stress rate changes from low to high ones. These phenomena are well predicted using the present model. Fig. 5 (b) shows the comparison of a stress-strain curve between the experimental results and theoretical predictions.
Measured and predicted tangent Young's moduli are reduced from 43.4 and 41.8 (for $300 < \sigma_x < 480$) to 36.7 and 37.1 GPa (for $480 < \sigma_x$), respectively. Difference in the Young's modulus for $300 < \sigma_x < 480$ is chiefly caused by the inverse nonlinearity of 0°-ply in the longitudinal direction which leads to a concave stress-strain curve.

Fig. 6 shows the comparison of the strains during the dead load tests between the experimental and predicted results. The predicted strain increases continuously because a continuous increase in the crack density is employed while the measured strains increase discontinuously. When the increase in transverse crack density is not taken into account, the estimated strain is much smaller than the measured one because the strain increment due to viscoelastic deformation is generated only in the early stage of the test. The predicted strain considering transverse cracking shows better agreement with the experimental results and the validity of the present model is verified through the above results.

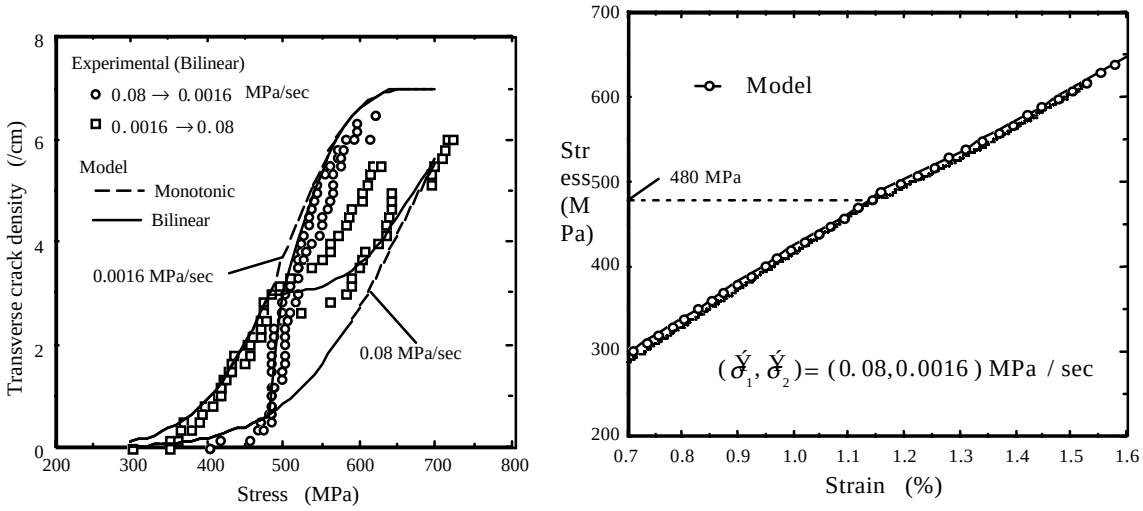

(a) (b)

Fig. 5: Measured and predicted (a) transverse crack density and (b) stress-strain curves during the bilinear tensile tests.

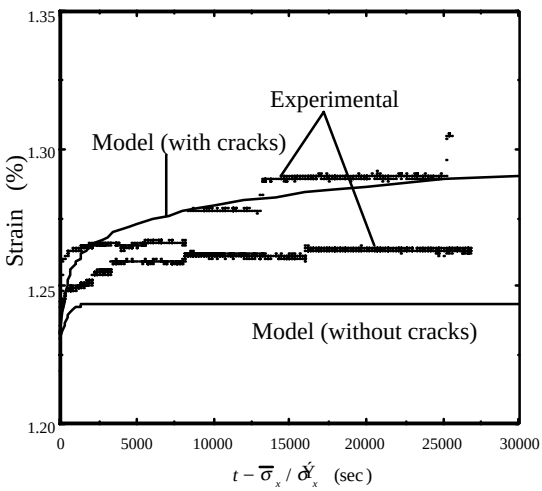

Fig. 6: Comparison of the strains during the dead load tests at 530 MPa between the experimental results and predictions.

CONCLUSIONS

A model is developed to predict the transverse crack density and strain response in cross-ply laminates under monotonic, bilinear and dead loading using the viscoelasticity theory, shear lag analysis and probabilistic failure model. The crack density and strain response under both bilinear and dead loading are predicted based on the above model using the parameters determined from the results of monotonic tensile tests. It is proved that the present model provides good agreement with the experimental results.

REFERENCES

1. Lou, Y. C. and Shapery, R. A., *J. Compos. Mater.*, **5** (1971), 208-234.
2. Horoschenkoff, A., *J. Compos. Mater.*, **24** (1990), 879-891.
3. Dillard, D. A., Morris, D. H. and Brinson, H. F., in: *Composite Materials: Testing and Design (Sixth Conference), ASTM STP 787*, Daniel, I. M. (ed.), American Society of Testing and Materials, Philadelphia, (1982), 357-370.
4. Flaggs, D. L. and Crossman, F. W., *J. Compos. Mater.*, **15** (1981), 21-40.
5. Chung, I., Sun, C. T. and Chang, I. Y., *J. Compos. Mater.*, **27** (1993), 1009-1029.
6. Manders, P. W., Chou, T.-W., Jones, F. R. and Rock, J. W., *J. Mater. Sci.*, **18** (1983), 2876-2889.
7. Fukunaga, H., Chou, T.-W., Peters, P. W. M. and Schulte, K., *J. Compos. Mater.*, **18** (1984), 339-356.
8. Peters, P. W. M., *J. Compos. Mater.*, **18** (1984), 545-556.
9. Lim, G. and Hong, C. S., *J. Compos. Mater.*, **23** (1989), 695-713.
10. Takeda, N. and Ogihara, S., *Compos. Sci. Tech.*, **52** (1994), 183-195.
11. Moore, R. H. and Dillard, D. A., *Compos. Sci. Technol.*, **39** (1990), 1-12.
12. Raghavan, J and Meshii, M., *Composites Part A* **27A** (1996), 1223-1227.
13. Ogi, K. and Takao, Y., *Advanced Compos. Mater.*, **8** (1999) (to be published).
14. Coleman, B. D., *J. Applied Phys.*, **29** (1958), 968-983.
15. Goda, K. and Hamada, J., *Materials Science Research International*, **2** (1996), 123-130.